DBL-1, a TGF-β, is essential for *Caenorhabditis elegans* aversive olfactory learning

Xiaodong Zhang[a] and Yun Zhang[b,1]

Departments of [a]Molecular and Cellular Biology and [b]Organismic and Evolutionary Biology, Center for Brain Science, Harvard University, Cambridge, MA 02138

Edited* by Cornelia Bargmann, Rockefeller University, New York, NY, and approved August 30, 2012 (received for review April 12, 2012)

The TGF-β superfamily is conserved throughout metazoan, and its members play essential roles in development and disease. TGF-β has also been implicated in adult neural plasticity. However, the underlying mechanisms are not well understood. Here we report that DBL-1, a *Caenorhabditis elegans* TGF-β homolog known to control body morphology and immunity, is essential for aversive olfactory learning of potentially harmful bacteria food. We show that DBL-1 generated by the AVA command interneurons, which are critical for sensorimotor responses, regulates aversive olfactory learning, and that the activity of the type I TGF-β receptor SMA-6 in the hypodermis is needed during adulthood to generate olfactory plasticity. These spatial and temporal mechanisms are critical for the DBL-1 signaling to achieve its diverse functions in development and adult neural plasticity. Interestingly, aversive training decreases AVA calcium response, leading to an increase in the DBL-1 signal secreted from AVA, revealing an experience-dependent change that can underlie the role of TGF-β signaling in mediating plasticity.

experience-dependent secretion | molecular and cellular mechanisms for TGF-beta pathway in learning

TGF-β ligands are secreted molecules that play critical roles in cell growth, differentiation, and death. TGF-βs initiate signaling by binding to type I and type II serine/threonine kinase receptors, which activate cytoplasmic SMAD proteins to regulate gene transcription (1). TGF-βs have also been implicated in adult neural plasticity (2–5). For example, in *Aplysia*, treating isolated pleural-pedal ganglia with human TGF-β1 induces long-term facilitation (5). In mice, removal of chordin, an extracellular inhibitor of BMPs (TGF-β family members), decreases the acquisition time for spatial learning in a Morris water maze (4). However, our understanding of TGF-β pathways in adult neural plasticity remains preliminary.

Caenorhabditis elegans is a great model organism for further exploring this question. The "wiring diagram" of the 302 neurons of its nervous system (6, 7) provides a structural basis for characterizing the function of TGF-β pathways that underlie learning. Two *C. elegans* TGF-β ligands have been well characterized: DAF-7 and DBL-1. Whereas DAF-7 regulates multiple physiological traits, including diapause stage (dauer) entry, metabolism (8–11), DBL-1 controls body morphology, innate immunity, and reproductive aging (9, 12, 13). Here we report that the activity of DBL-1 is critical for adult animals to learn to avoid the smell of pathogenic bacteria. DBL-1 produced by the AVA command interneurons mediates learning, and the type I TGF-β receptor SMA-6 acts primarily in the hypodermis during adulthood to facilitate olfactory plasticity. These spatial and temporal mechanisms are critical for the diverse functions of the DBL-1/SMA-6 pathway. Interestingly, aversive training with pathogenic bacteria represses AVA activity measured by G-CaMP, and inhibition of AVA leads to an increased amount of DBL-1 secreted by AVA, revealing an experience-dependent change of DBL-1 that may underlie its role in neural plasticity.

Results

***C. elegans* TGF-β/DBL-1 Is Essential for Aversive Olfactory Learning in Adult Animals.** *C. elegans* feeds on bacteria and detects odorants produced by bacteria (14). Whereas many bacteria in its habitat can be safely ingested by *C. elegans*, some strains are pathogenic, and ingestion of these stains could cause a slow death over several days (15). Previously we showed that adult *C. elegans* is able to learn to avoid the smell of pathogenic bacteria after ingestion (16, 17). Here we quantified this learning ability using a short-term training procedure. We raised animals under standard conditions until adulthood, then transferred half of the animals onto a control plate containing the benign bacteria strain *Escherichia coli* OP50 and the other half onto a training plate containing the pathogenic strain *Pseudomonas aeruginosa* PA14. After 4 h, the naive animals on the control plate and the trained animals exposed to PA14 were tested in parallel to determine their preferences between OP50 and PA14 in the choice assays similar to the chemotaxis assays with odorants (14) (Fig. 1*A*). Animals orient their locomotion toward a small lawn of freshly resuspended OP50 or PA14 culture over a distance, likely by detecting volatiles, "the smell," produced by the bacteria. This results in accumulation of the animals on either bacteria lawn over a time course of 1–2 h, and the choice between OP50 and PA14 was measured using a choice index. A positive choice index indicates a preference for PA14, and a negative choice index indicates a preference for OP50 (Fig. 1 *A* and *B* and Fig. S1*A*).

We found that naive adult animals that were never exposed to PA14 slightly preferred or were indifferent to the smell of PA14, whereas animals trained with a 4-h exposure to PA14 strongly avoided the strain (Fig. 1 *A* and *B* and Fig. S1*A*). The induced avoidance of PA14 was robust whether OP50 was used as a control in two-choice assays or several different bacterial strains were used as controls in multiple-choice assays (16). The learning index was the difference between the choice indices of the naive and trained animals, and a positive learning index indicates a learned olfactory aversion to PA14 (Fig. 1 *B* and *C*). Similarly, short exposure to another pathogenic bacterium, *Serratia marcescens* ATCC 13880, induced an aversive learning in adults. In contrast, exposure to nonpathogenic bacteria, such as *Pseudomonas fluorescens* and *P. aeruginosa* PAK, did not cause olfactory aversion (Fig. 1*C*). These results demonstrate that a short-term training with pathogenic bacteria induces aversive olfactory learning in adult animals.

Next, using the short-term training with the pathogenic bacterium PA14, we found that two loss-of-function mutations in *dbl-1*, *dbl-1(nk3)* and *dbl-1(wk70)* (18, 19), disrupted aversive learning (Fig. 1*D*). Introduction of the *dbl-1* genomic DNA rescued the defects of *dbl-1(nk3)* mutant animals in learning and body length (Fig. 2 *A*, *G*, and *H*). *dbl-1(nk3)* mutant animals were also defective in learning to avoid the pathogen *S. marcescens* 13880 (Fig. S1*B*). Meanwhile, the chemotactic responses of *dbl-1(nk3)* mutant animals to odorants detected by the primary olfactory neurons (14) are similar to wild-type animals, or even stronger toward octanol (Fig. S2). Thus, DBL-1 is required

Author contributions: X.Z. and Y.Z. designed research; X.Z. performed research; X.Z. and Y.Z. analyzed data; and X.Z. and Y.Z. wrote the paper.

The authors declare no conflict of interest.

*This Direct Submission article had a prearranged editor.

[1]To whom correspondence should be addressed. E-mail: yzhang@oeb.harvard.edu.

This article contains supporting information online at www.pnas.org/lookup/suppl/doi:10.1073/pnas.1205982109/-/DCSupplemental.

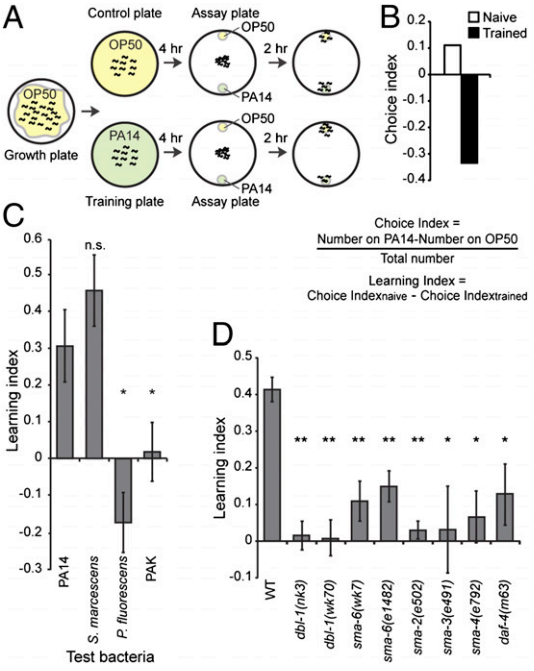

Fig. 1. DBL-1 pathway is essential for aversive olfactory learning. (*A*) Short-term training procedure for aversive olfactory learning. (*B*) Sample choice indices. (*C*) Learning indices of wild-type (WT) animals trained with different bacteria, compared with the learning index of PA14. (*D*) Mutations in the DBL-1 pathway impair aversive olfactory learning of PA14. For *C* and *D*, Student *t* test, $^{**}P < 0.01$, $^{*}P < 0.05$; n.s., $P > 0.05$; $n \geq 3$ assays, error bars represent SEM.

for aversive olfactory learning of pathogenic bacteria in *C. elegans*. DBL-1 signals through the type I receptor SMA-6 and the type II receptor DAF-4 to control body morphology (20). We found that *sma-6(e1482)*, *sma-6(wk7)* (21), *daf-4(m63)*, and mutant animals of SMAD proteins, *sma-2(e502)*, *sma-3(e491)*, and *sma-4(e792)* (9, 22), were all defective in learning avoidance of PA14 (Fig. 1*D*). The residual learning ability in the *sma-6 (e1482)* may be due to the weak mutation in the allele (21). Thus, the TGF-β/DBL-1 pathway is essential for aversive olfactory learning of pathogenic bacteria in adult animals.

DBL-1 Produced by the AVA Command Interneurons Promotes Aversive Olfactory Learning. Next we sought the neuronal source of the DBL-1 signal for learning regulation. First, using transcriptional and translational reporters (Fig. S3*A*), we confirmed *dbl-1* expression in the nervous system, including ventral nerve cord (VNC) motor neurons (18, 19). Interestingly, we also identified *dbl-1* expression in the AVA command interneurons on the basis of the anatomical position and overlapping expression of *dbl-1* with the glutamate receptor *nmr-1* (23) (Fig. 2*B* and Fig. S3*B*).

The AVA interneurons are important to initiate backward movements (23–26). We found that expression of the *dbl-1* coding region using the *nmr-1* promoter, whose expression overlaps with *dbl-1* expression only in AVA, significantly rescued the learning defect in *dbl-1(nk3)* mutant animals (Fig. 2 *C* and *G*). To selectively express *dbl-1* in AVA neurons, we used the Cre-Lox recombination system (27) by expressing two transgenes, *flp-18p::nCre* and *nmr-1sp::LoxStopLox::dbl-1*, which direct Cre-mediated deletion of the Stop signal only in AVA neurons (Fig. S3*C*). The AVA-specific expression was validated by the coexpression of the *flp-18p::nCre* and *nmr-1sp::LoxStopLox::gfp* constructs (Fig. S3 *D* and *E*). Consistently, AVA-specific expression of *dbl-1* rescued the learning defect of *dbl-1(nk3)* mutant animals (Fig. 2*D*). We also tested the effect of *dbl-1* expression in the VNC motor neurons. The *unc-17* promoter is active in many neurons, including those in VNC, but not AVA; and the *acr-2* promoter expresses mainly in the *dbl-1*–expressing VNC motor neurons (28) (Fig. 2*G*). Neither *unc-17p::dbl-1* nor *acr-2p::dbl-1* significantly improved the learning ability of *dbl-1(nk3)* animals (Fig. 2 *E* and *F*). Thus, the DBL-1 signal produced by the AVA interneurons mediates aversive olfactory learning.

DBL-1 also regulates body morphology and immunity. *dbl-1* mutant animals are smaller and more susceptible to infection (13, 18, 19, 29). We found that *dbl-1* expression in AVA using the *nmr-1* promoter rescued only the learning defect of *dbl-1(nk3)* mutant animals and had no obvious effect on body length or resistance to PA14 (Fig. 2 *C*, *H*, and *I* and Table S1). Killing of *C. elegans* by PA14 correlates with the accumulation of PA14 in the gut (15). Consistently, expression of *dbl-1* with *nmr-1p* could not rescue the increased accumulation of DsRed-labeled PA14 in the gut of *dbl-1(nk3)* animals (Fig. S4*A*). In contrast, expressing *dbl-1* in mutant animals using the *unc-17* promoter restored body length and resulted in stronger resistance to PA14 than in wild-type animals without significantly improving their learning ability (Fig. 2 *E*, *H*, and *I* and Table S1). Thus, DBL-1 ligands produced by different neurons regulate distinct physiological processes.

DBL-1 Signals to the Hypodermis to Direct Aversive Olfactory Learning. DBL-1 acts on the type I receptor SMA-6 in the hypodermis to regulate body length (30). We find that SMA-6 is also required for aversive learning of PA14 (Fig. 1*D*), and expression of a wild-type *sma-6* transgene rescued the learning defect of *sma-6(wk7)* mutant animals (Fig. 3*A*). By examining the expression pattern of a GFP reporter of *sma-6*, we confirmed expression of *sma-6* in the pharynx, intestine, and hypodermis (30). We also identified *sma-6* expression in the ASI sensory neurons (Fig. S4*B*), using DiI that stains several ciliated neurons, including ASI.

Next, we expressed wild-type SMA-6 selectively in the hypodermis, intestine, or ASI neurons in *sma-6(wk7)* mutant animals using cell-specific promoters and assessed its ability to rescue the learning defect (Fig. 3*G*). We found that expression of *sma-6* either in the hypodermis [*dpy-7p::sma-6(low)*, *col-12p::sma-6*] or in the ASI neurons (*str-3p::sma-6*) fully rescued the learning defect of *sma-6(wk7)* animals (Fig. 3 *B–D*). In contrast, expression of *sma-6* in the intestine (*elt-2p::sma-6*, *ges-1p::sma-6*) had no detectable effect on learning (Fig. 3 *E* and *F*). Thus, the activity of SMA-6 receptor in either the hypodermis or ASI neurons is sufficient for aversive olfactory learning. Next, we blocked SMA-6 signaling in these regions using SMA-6(Δk), a dominant-negative isoform that lacks the intracellular kinase domain. Mutations disrupting the kinase domain of TGF-β receptors inhibit signal transduction of the corresponding pathway (31). Expression of *sma-6(Δk)* using the hypodermis-specific promoter *dpy-7* in the wild-type animals resulted in decreased body length, similar to the phenotype of *sma-6(wk7)* mutant animals (Fig. S4*C*), confirming the dominant-negative effect of SMA-6(Δk). Consequently, we found that blocking SMA-6 signaling in the hypodermis [*col-19p::sma-6(Δk)*] (32) of wild-type animals strongly impaired aversive learning, whereas expression of *sma-6(Δk)* in ASI [*str-3p::sma-6(Δk)*] had no detectable effect (Fig. 3 *H* and *I*). Thus, the hypodermis is the primary functional site of SMA-6 in aversive olfactory learning.

DBL-1/SMA-6 Pathway Acts in Adults to Facilitate Aversive Olfactory Learning. We next investigated when the DBL-1 pathway is required for the adult-stage learning. We blocked DBL-1 signal transduction in wild-type animals by expressing the dominant-negative SMA-6(Δk) right before adult stage using the heat shock-inducible promoter *hsp16.2p*. We found that the transgenic animals were completely defective in aversive learning, whereas the nontransgenic siblings that went through the same heat shock treatment were normal (Fig. 4*A*). Conversely, when we expressed wild-type SMA-6 in the hypodermis of *sma-6(wk7)* mutant animals only during adulthood using the adult-specific promoter *col-19p* (32), the learning defect was significantly rescued (Fig. 4*B*). Thus, the function of the DBL-1/SMA-6 pathway during adult stage is critical for aversive olfactory learning.

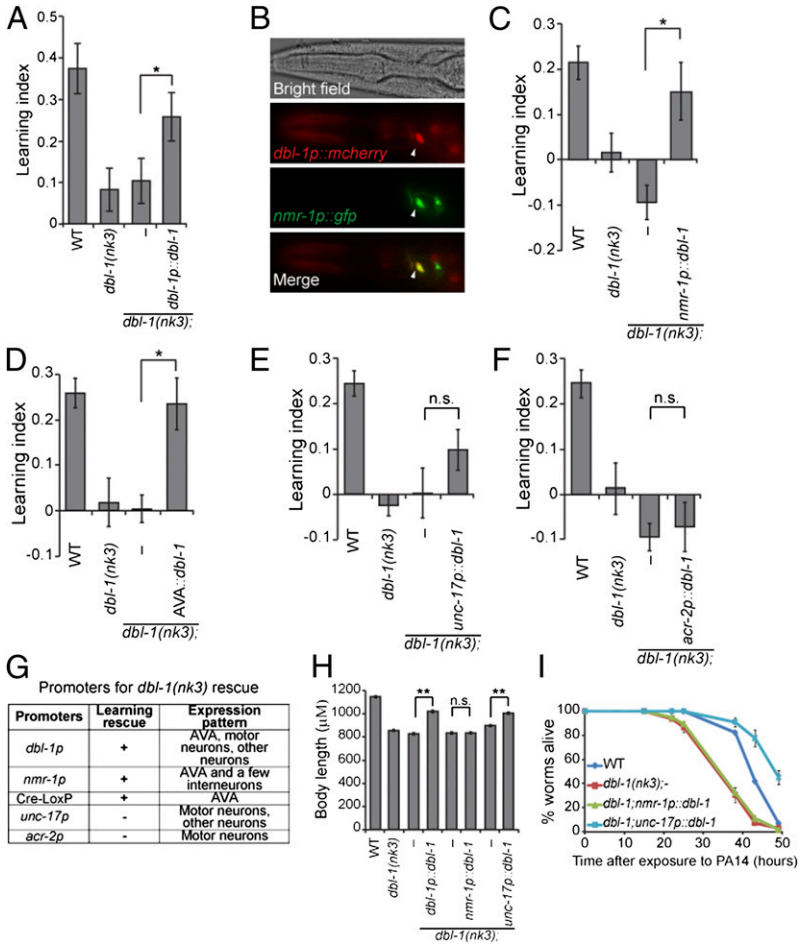

Promoters	Learning rescue	Expression pattern
dbl-1p	+	AVA, motor neurons, other neurons
nmr-1p	+	AVA and a few interneurons
Cre-LoxP	+	AVA
unc-17p	-	Motor neurons, other neurons
acr-2p	-	Motor neurons

Fig. 2. DBL-1 produced by the AVA interneurons mediates aversive olfactory learning. (*A*) *dbl-1* genomic DNA rescues the learning defect of *dbl-1(nk3)* animals ($n = 11$ assays). (*B*) *dbl-1* is expressed in the AVA (arrowheads). (*C–F*) Expression of *dbl-1* using the *nmr-1* promoter (*C*, $n = 6$ assays) or the AVA-selective expression of *dbl-1* (*D*, $n = 11$ assays) rescues the learning defect of *dbl-1(nk3)* animals, but expression of *dbl-1* using the *unc-17* promoter (*E*, $n = 13$ assays) or the *acr-2* promoter (*F*, $n = 6$ assays) does not rescue. (*G*) Promoters used in the *dbl-1* rescue experiments. (*H*) Body length measurement ($n \geq 26$ animals for each genotype). In *A*, *C–F*, and *H*, transgenic animals were compared with nontransgenic siblings using the paired Student *t* test (**$P < 0.01$, *$P < 0.05$; n.s., $P > 0.05$; error bars represent SEM). (*I*) Representative individual slow-killing assays with the pathogenic bacterium PA14 ($n \geq 3$ assays for each genotype, $n \geq 3$ replicates in each assay; error bars represent SEM; Kaplan-Meier procedure and log–rank test; Table S1).

NEUROSCIENCE

Because SMA-6 also acts in the hypodermis to control body size and pathogen resistance (13, 30, 33), we asked how the DBL-1/SMA-6 signaling regulates these diverse physiological traits. We found that a low level of SMA-6 expression in the hypodermis [*dpy-7p::sma-6(low)*] was sufficient to rescue the defect of *sma-6(wk7)* animals in learning (Fig. 3*B*) but not sufficient to rescue their defect in pathogen resistance or body length; these phenotypes required a higher level of SMA-6 expression in hypodermis [*dpy-7p::sma-6(high)*] for rescue (Fig. 4 *C–E* and Table S1). Consistently, only a higher level of hypodermal SMA-6 was able to rescue the increased accumulation of PA14/DsRed in the gut of *sma-6 (wk7)* animals (Fig. S4*A*). In addition, adult-stage expression of

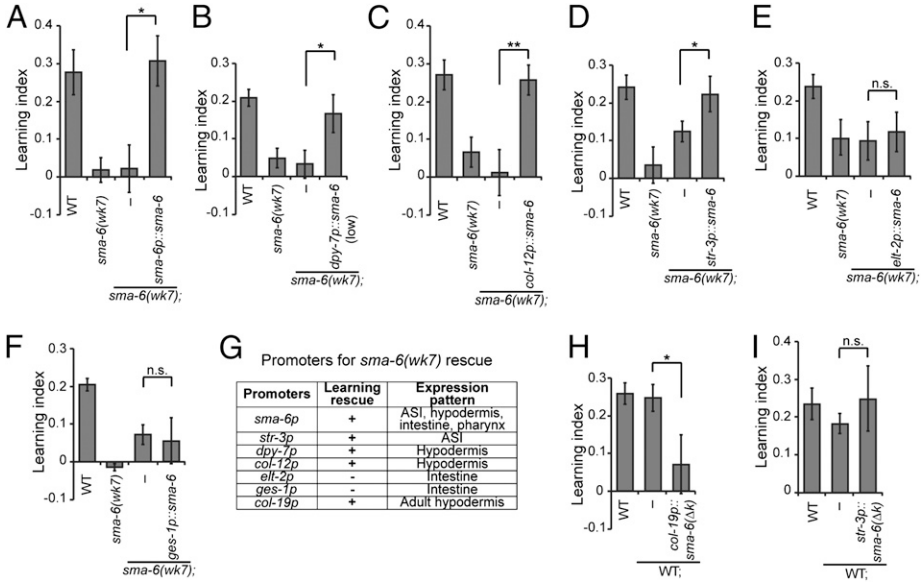

Promoters	Learning rescue	Expression pattern
sma-6p	+	ASI, hypodermis, intestine, pharynx
str-3p	+	ASI
dpy-7p	+	Hypodermis
col-12p	+	Hypodermis
elt-2p	-	Intestine
ges-1p	-	Intestine
col-19p	+	Adult hypodermis

Fig. 3. SMA-6 receptor acts in the hypodermis to facilitate aversive olfactory learning. (*A*) Genomic DNA of *sma-6* rescues the learning defect of *sma-6(wk7)* mutant animals. (*B–F*) Expression of wild-type *sma-6* in the hypodermis (*B* and *C*) or in the ASI neurons (*D*) rescues the learning defect of *sma-6(wk7)* animals, but expression of wild-type *sma-6* in the intestine (*E* and *F*) does not rescue. (*G*) Promoters used in *sma-6* rescue experiments. (*H* and *I*) Blocking DBL-1/SMA-6 signaling by expressing the dominant-negative *sma-6*(Δ*k*) in the hypodermis (*H*) of wild-type animals impairs learning, but blocking DBL-1/SMA-6 signaling in ASI (*I*) has no effect. In *A–F*, *H*, and *I*, transgenic animals and nontransgenic siblings were compared using the paired Student *t* test (**$P < 0.01$, *$P < 0.05$; n.s., $P > 0.05$; $n \geq 5$ assays; error bars represent SEM).

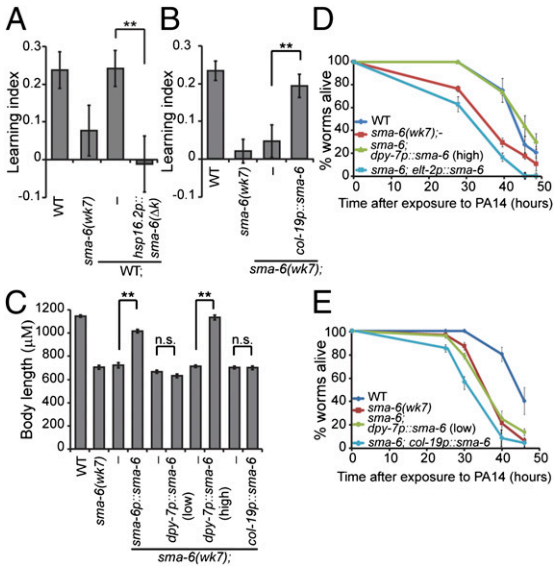

Fig. 4. DBL-1/SMA-6 pathway acts during adulthood for aversive olfactory learning. (*A*) Blocking DBL-1/SMA-6 signaling at a late developmental stage abolishes the learning ability of wild-type animals ($n = 6$ assays). (*B*) Adult-specific expression of wild-type *sma-6* activity in the hypodermis rescues the learning defect of *sma-6(wk7)* animals ($n = 13$ assays). (*C*) Body length measurements ($n \geq 23$ animals each genotype). In *A*–*C*, transgenic animals were compared with nontransgenic siblings using the paired Student *t* test (**$P < 0.01$; n.s., $P > 0.05$; error bars represent SEM). (*D* and *E*) Representative individual slow-killing assays with the pathogenic bacterium PA14 ($n \geq 3$ assays for each genotype, $n \geq 3$ replicates in each assay; error bars represent SEM; Kaplan-Meier procedure and log–rank test; Table S1).

SMA-6 in the hypodermis (*col-19p::sma-6*) exerted no obvious effect on body length or pathogen resistance, although it significantly rescued the learning defect in *sma-6(wk7)* animals (Fig. 4 *B*, *C*, and *E* and Table S1). These results suggest that dosage and temporal patterns are important for the DBL-1/SMA-6 pathway to mediate diverse functions.

Aversive Training Decreases AVA Neuronal Calcium Response. To understand how the DBL-1 signal from AVA mediates learning, we examined whether aversive training alters AVA neuronal activity. We measured the calcium response of AVA neurons using intracellular calcium imaging in transgenic animals that expressed the calcium-sensitive fluorescent protein G-CaMP with the *nmr-1* promoter (34). These transgenic animals display normal learning ability and locomotory responses (Fig. S5 *A* and *B*). Because calcium influx of AVA is correlated with the initiation of spontaneous backward movements (26, 35, 36), we recorded AVA calcium dynamics of animals in the nematode growth medium (NGM) buffer using a microfluidic device that allows generation of body waves, which result in forward or backward movements (36). We measured the G-CaMP fluorescence intensity in AVA in naive and PA14-trained animals and calculated the rate of intensity change (Fig. 5*A*). We determined calcium influx events in AVA by identifying peaks of intensity change rate that were above a given threshold. Interestingly, trained animals displayed significantly lower frequencies of calcium influx events in AVA than naive animals over a range of thresholds (Fig. 5 *B* and *C*). To control for motion artifacts, we used the same procedure to quantify GFP signal in AVA and did not detect obvious peaks ("Control" in Fig. 5*C*). Previously we showed that training with PA14 did not alter sensory-evoked calcium responses in the AWB and AWC sensory neurons (17). These results suggest that aversive training reduces AVA calcium response.

Because animals lacking AVA neurons initiate fewer reversals on food (23–25), we confirmed the training-dependent decrease in AVA calcium response by measuring reversal rates. We quantified short reversals (one or two head swings), long reversals (more than two head swings), and omega turns (animal bends its body into a Ω shape). We found that compared with naive animals on OP50, trained animals generated fewer reversals on PA14 (Fig. 5*D*), which may facilitate the leaving and/or avoiding PA14 bacterial lawn in trained animals. In addition, the reduction in reversal rates was not observed on the nonpathogenic derivative strain PA14 *gacA*$^-$ (Fig. 5*E*). These results further indicate that aversive training decreases AVA calcium response.

Aversive Training Increases the DBL-1 Signal Secreted by the AVA Interneurons. The above observation prompted us to investigate the effect of training on AVA production of DBL-1. First, we found that 4- to 6-h training increases the expression of the *dbl-1p::mcherry* transcriptional reporter in AVA (Fig. 6*A*). This increase was not observed with 2-h exposure or in VNC motor neurons (Fig. S5*C*), suggesting that the increase in *dbl-1* transcription is contingent on continuing training beyond the initial contact of the bacteria and is specific to AVA. Next, we examined whether the DBL-1 signal secreted by AVA neurons is also modulated by training using a translational reporter *gfp::dbl-1*. The reporter is functional because expression of *gfp::dbl-1* using the *dbl-1* promoter rescues both the body length and learning defects of *dbl-1(nk3)* mutant animals (Fig. S5 *D* and *E*). We expressed the functional GFP::DBL-1 protein only in AVA neurons using the Cre-Lox strategy as in the *dbl-1* rescue experiment (Fig. S5*F*). We first confirmed that the promoters used to drive AVA-specific expression of GFP::DBL-1, *nmr-1sp*, and *flp-18p* were not regulated by training by measuring the expression of their GFP transcriptional reporters (Fig. 6*B*). Next, we measured the amount of secreted GFP::DBL-1 by quantifying the intensity of green fluorescent patches inside coelomocytes. Coelomocytes are scavenger cells that take up secreted proteins from the pseudocoelomic space through endocytosis (37). Thus, the fluorescent patches of GFP::DBL-1 that accumulate in the coelomocytes (Fig. 6*C*) indicate the level of secreted GFP::DBL-1. In this study, we also measured the mean fluorescence intensity of the entire coelomocytes and obtained similar results (Figs. 6 and 7 and Fig. S6). We found that, compared with naive

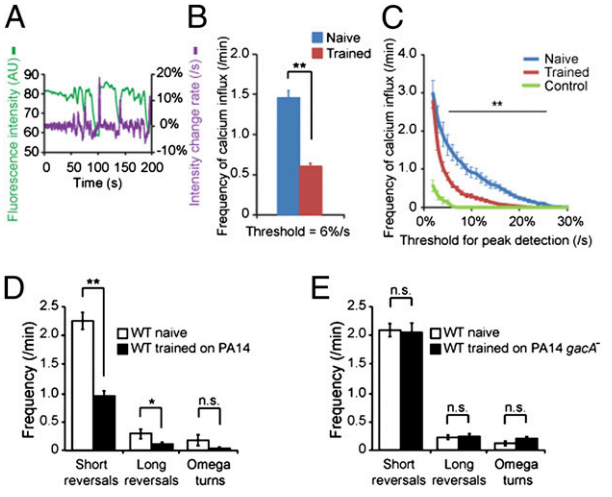

Fig. 5. Aversive training decreases AVA calcium response. (*A*) Sample traces for AVA calcium imaging. The G-CaMP signal is green; the rate of G-CaMP intensity change is purple (AU, arbitrary unit). (*B* and *C*) Trained animals display fewer calcium influx events in AVA at one threshold (*B*) or across a range of thresholds (*C*). Control, GFP signal in AVA. In *B* and *C*, Student *t* test, **$P < 0.01$; $n \geq 42$ animals each condition, $n = 12$ for control; error bars represent SEM. (*D* and *E*) Reversal rates displayed by naive and PA14-trained wild-type animals (*D*, $n = 11$ animals each condition) or by naive and PA14 *gacA*$^-$-trained wild-type animals (*E*, $n = 8$ animals each). (Student *t* test, **$P < 0.01$, *$P < 0.05$; n.s., $P > 0.05$; error bars represent SEM).

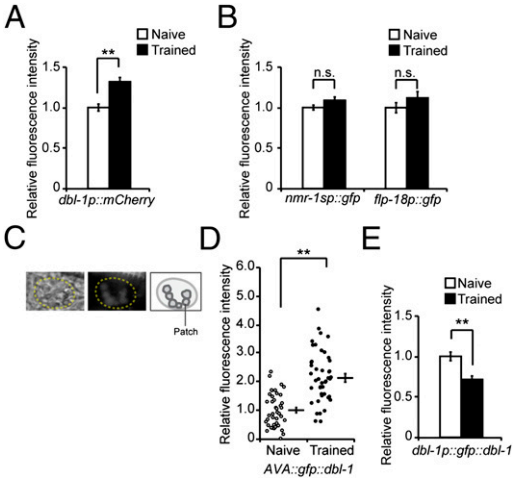

Fig. 6. Aversive olfactory training increases the DBL-1 signal secreted from AVA. (*A*) Expression of a *dbl-1* transcriptional reporter in AVA increases after training with PA14 (Student *t* test, $^{**}P < 0.01$; $n \geq 100$ animals each condition; error bars represent SEM). (*B*) *nmr-1sp* and *flp-18p* are stable during training (Student *t* test; n.s., $P > 0.05$; $n \geq 29$ animals each; error bars represent SEM). *nmr-1sp*: a shorter version of *nmr-1p*. (*C*) Sample images and schematics for coelomocytes and the accumulation of AVA-secreted GFP::DBL-1 fluorescent patches in the coelomocytes. (*D*) Training increases accumulation of AVA-secreted GFP::DBL-1 in coelomocytes. The GFP::DBL-1 fluorescent patches in coelomocytes were quantified (circles or dots: individual measurements; Student *t* test, $^{**}P < 0.01$; $n \geq 41$ animals each condition; error bars represent SEM). (*E*) Expression of *dbl-1p::gfp::dbl-1* decreases in AVA neurons after training (Student *t* test, $^{**}P < 0.01$; $n \geq 103$ animals each; error bar represents SEM). In *A*, *B*, *D*, and *E*, the fluorescence signals were normalized using the signals from naive animals as the baseline.

animals, animals trained with PA14 showed significantly stronger GFP::DBL-1 fluorescence in coelomocytes (Fig. 6*D* and Fig. S6*A*). Similar up-regulation was observed in another two independently generated transgenic lines (Fig. S6 *B* and *C*). Furthermore, the expression of the translational fusion *dbl-1p::gfp::dbl-1* decreased in AVA after training, consistent with an increase in the secretion of DBL-1 from AVA (Fig. 6*E*). As a control, we quantified the fluorescent signals produced by a translational fusion *lad-2p::ss-mcherry*. *lad-2* encodes a cell adhesion molecule expressed in several neurons (38), and fusing the LAD-2 signal peptide (*ss*) with mCherry produced a secreted protein. There was no difference in the fluorescent signals of *lad-2p::ss-mcherry* either in the *lad-2*–expressing head neurons or in coelomocytes between naive and trained animals (Fig. S6 *D* and *E*), suggesting that training does not significantly alter the uptake function of coelomocytes. Together, these results demonstrate that aversive training causes an increase in the amount of DBL-1 ligand secreted by the AVA neurons.

To further assess the training effect on DBL-1 signaling, we examined the downstream activity in the hypodermis, the target tissue of DBL-1 in aversive olfactory learning, using a *gfp* reporter of DBL-1 activity, RAD-SMAD (39). RAD-SMAD expression is positively regulated by DBL-1 and is found in multiple tissues, including the intestine and hypodermis (39). We quantified RAD-SMAD level in the hypodermis of transgenic animals that expressed DBL-1 only in AVA neurons in the *dbl-1(nk3)* background. To control for individual variations and unspecific effects, we normalized the hypodermal RAD-SMAD signal by the intestinal signal of the same animal. We found that training with PA14 enhanced RAD-SMAD expression in the hypodermis (Fig. 7*A*). In contrast, exposure to a nonvirulent *Pseudomonas* strain, PAK, which does not induce aversive learning (Fig. 1*C*), did not generate a similar increase (Fig. S6*F*). Because AVA is the only source of DBL-1 in this condition, this result supports that aversive training with PA14 increases the DBL-1 signal from AVA neurons.

Although training decreases AVA neuronal activity measured by G-CaMP signal, it increases AVA-secreted DBL-1 signal. Thus, we tested whether there was a causal link between these two effects. We inhibited AVA in wild-type animals by selectively expressing an activated form of a potassium channel *twk-18(gf)* (40) in AVA. We observed strongly decreased reversal rates in these transgenic animals, confirming the inhibition of AVA (Fig. 7*B*) (25). Strikingly, in the absence of training this TWK-18–mediated inhibition of AVA generated a significant increase in the AVA-secreted GFP::DBL-1 signal, as measured using the coelomocyte-uptake assay (Fig. 7*C* and Fig. S6*G*). These results demonstrate that inhibition of AVA could lead to an increased amount of DBL-1 signal secreted by the AVA interneurons.

Discussion

Growth factors involved in early development also mediate adult neural plasticity (41, 42). The TGF-β superfamily regulates development and disease in a conserved manner. Here we elucidate an essential requirement for the pathway of *C. elegans* TGF-β homolog DBL-1 in regulating aversive olfactory learning. Occasionally mutations in DBL-1 pathway also affect the naive preference, suggesting potential function of the pathway under the naive condition. Our results demonstrate the specific role of DBL-1 produced by the AVA command interneurons in facilitating learning by acting through the SMA-6 receptor in the adult hypodermis. The cell bodies of AVA neurons are located in the head, and their processes run along the length of the animal, embedded in the hypodermis. Although we cannot completely exclude the possibility that DBL-1 produced by some other cells can also act on the hypodermal SMA-6 through diffusion in pseudocoelom, our results suggest that the DBL-1 secreted by AVA neurons activates the SMA-6 receptor in the surrounding

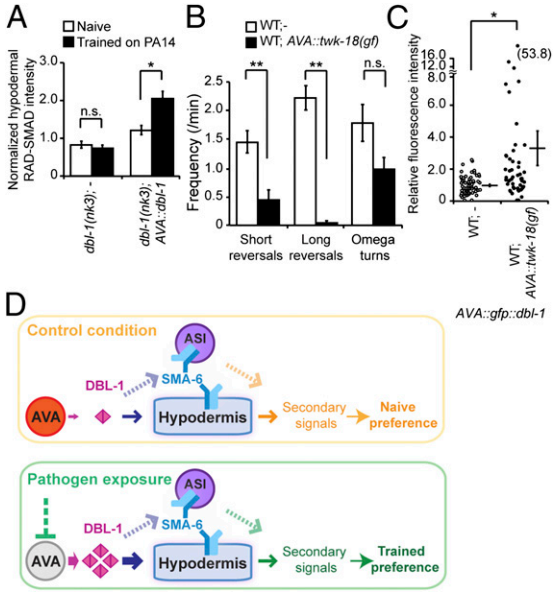

Fig. 7. Decreased AVA neuronal activity causes an increase in the amount of DBL-1 secreted by AVA. (*A*) Training enhances the hypodermal RAD-SMAD activity in animals that express *dbl-1* only in AVA neurons in *dbl-1 (nk3)* mutant background (Student *t* test, $^{*}P < 0.05$; n.s., $P > 0.05$; $n \geq 77$ animals each; error bars represent SEM). (*B*) AVA-specific expression of a potassium channel *twk-18(gf)* decreases reversal rates (Student *t* test, $^{**}P < 0.01$; n.s., $P > 0.05$; $n = 8$ animals each; error bars represent SEM). (*C*) AVA-specific expression of *twk-18(gf)* increases GFP::DBL-1 secreted from AVA in animals that express GFP::DBL-1 only in AVA. The GFP::DBL-1 patches inside coelomocytes were measured, and signals were normalized using the signals from wild-type (WT) animals as the baseline (circles or dots: individual measurements; Student *t* test, $^{*}P < 0.05$; $n \geq 51$ animals each; error bar represents SEM). (*D*) Working model.

hypodermis to elicit secondary signaling to induce aversive learning. DBL-1 also acts via the hypodermis to regulate body length and pathogen resistance (9, 13, 30). Thus, the hypodermis may act as a general target tissue for DBL-1 signals.

Command interneurons are necessary and sufficient to generate defined behavioral outputs. In the mollusc *Pleurobranchaea*, pairing food with shock results in postsynaptic modulation of the PCN command neurons, which activate feeding upon food stimuli (43). Here we demonstrate the requirement of the AVA command interneurons as the source of DBL-1 that is needed for a learning behavior. Interestingly, aversive training with PA14 decreases AVA neuronal calcium signal but increases the amount of DBL-1 secreted by AVA. In the rat supraoptic nucleus, administration of α-melanocyte–stimulating hormone decreases the electrical activity of oxytocin-containing neurons and the axonal release, while increasing the dendritic release of oxytocin (44). One plausible physiological consequence of the training-dependent change in secreted DBL-1 would be an enhanced signal to SMA-6, which could result in modulation of a secondary signal, leading to behavioral changes (Fig. 7*D*).

TGF-β pathways regulate diverse physiological processes. Recent studies demonstrated that individual TGF-βs can activate different receptor complexes and downstream effectors to elicit distinct responses (1). Our results argue that TGF-β secreted by different cells/tissues at different times can induce distinct physiological effects. Elucidation of the mechanisms used by target tissues to interpret these diverse TGF-β signals awaits future investigation.

Materials and Methods

SI Materials and Methods provides full experimental details. For the promoters used in transgenic lines, we found no significant impact of their expression on learning using the corresponding fluorescent reporters and the transformation marker (Table S2). The aversive olfactory training and learning assays were performed similarly as previously described (16, 17). For transgenic lines, the transgenic and nontransgenic siblings were trained on the same plates, their learning ability was measured in the same chemotaxis assays, and the results were scored by the experimenter before the genotypes were identified according to the expression of a fluorescent transformation maker in transgenic animals. The results of all of the choice indices are in Table S3.

ACKNOWLEDGMENTS. We thank the *Caenorhabditis* Genetics Center, which is funded by the National Institutes of Health (NIH) National Center for Research Resources, for strains; Wellcome Trust Sanger Institute for DNA clones; Fred Ausubel for PA14/DsRed; Edward Soucy and Parker Porfilio for technical support; Queelim Ch'ng for suggestions on imaging coelomocytes; Junichi Nakai for pN1-G-CaMP; Jingyi Yu for the *flp-18p* and *unc-17p* constructs; and Xu Zhou for calcium imaging analysis. This work was supported by the Esther A. and Joseph Klingenstein Fund, the March of Dimes Foundation, the Alfred P. Sloan Foundation, The John Merck Fund, and by NIH Grant R01 DC009852 (to Y.Z.).

1. Moustakas A, Heldin CH (2009) The regulation of TGFbeta signal transduction. *Development* 136:3699–3714.
2. Ageta H, et al. (2010) Activin plays a key role in the maintenance of long-term memory and late-LTP. *Learn Mem* 17:176–185.
3. Goold CP, Davis GW (2007) The BMP ligand Gbb gates the expression of synaptic homeostasis independent of synaptic growth control. *Neuron* 56:109–123.
4. Sun M, et al. (2007) Presynaptic contributions of chordin to hippocampal plasticity and spatial learning. *J Neurosci* 27:7740–7750.
5. Zhang F, Endo S, Cleary LJ, Eskin A, Byrne JH (1997) Role of transforming growth factor-β in long-term synaptic facilitation in *Aplysia*. *Science* 275:1318–1320.
6. White JG, Southgate E, Thomson JN, Brenner S (1986) The structure of the nervous system of the nematode *Caenorhabditis elegans*. *Phil Trans R Soc London B* 314: 1–340.
7. Chen BL, Hall DH, Chklovskii DB (2006) Wiring optimization can relate neuronal structure and function. *Proc Natl Acad Sci USA* 103:4723–4728.
8. Greer ER, Pérez CL, Van Gilst MR, Lee BH, Ashrafi K (2008) Neural and molecular dissection of a *C. elegans* sensory circuit that regulates fat and feeding. *Cell Metab* 8: 118–131.
9. Savage-Dunn C (2005) TGF-β signaling. *Wormbook*, 10.1895/wormbook.1.22.1. Available at http://www.wormbook.org.
10. You YJ, Kim J, Raizen DM, Avery L (2008) Insulin, cGMP, and TGF-β signals regulate food intake and quiescence in *C. elegans*: A model for satiety. *Cell Metab* 7:249–257.
11. Chang AJ, Chronis N, Karow DS, Marletta MA, Bargmann CI (2006) A distributed chemosensory circuit for oxygen preference in *C. elegans*. *PLoS Biol* 4:e274.
12. Luo S, Kleemann GA, Ashraf JM, Shaw WM, Murphy CT (2010) TGF-β and insulin signaling regulate reproductive aging via oocyte and germline quality maintenance. *Cell* 143:299–312.
13. Zugasti O, Ewbank JJ (2009) Neuroimmune regulation of antimicrobial peptide expression by a noncanonical TGF-β signaling pathway in *Caenorhabditis elegans* epidermis. *Nat Immunol* 10:249–256.
14. Bargmann CI, Hartwieg E, Horvitz HR (1993) Odorant-selective genes and neurons mediate olfaction in *C. elegans*. *Cell* 74:515–527.
15. Tan MW, Mahajan-Miklos S, Ausubel FM (1999) Killing of *Caenorhabditis elegans* by *Pseudomonas aeruginosa* used to model mammalian bacterial pathogenesis. *Proc Natl Acad Sci USA* 96:715–720.
16. Zhang Y, Lu H, Bargmann CI (2005) Pathogenic bacteria induce aversive olfactory learning in *Caenorhabditis elegans*. *Nature* 438:179–184.
17. Ha HI, et al. (2010) Functional organization of a neural network for aversive olfactory learning in *Caenorhabditis elegans*. *Neuron* 68:1173–1186.
18. Morita K, Chow KL, Ueno N (1999) Regulation of body length and male tail ray pattern formation of *Caenorhabditis elegans* by a member of TGF-β family. *Development* 126:1337–1347.
19. Suzuki Y, et al. (1999) A BMP homolog acts as a dose-dependent regulator of body size and male tail patterning in *Caenorhabditis elegans*. *Development* 126:241–250.
20. Estevez M, et al. (1993) The *daf-4* gene encodes a bone morphogenetic protein receptor controlling *C. elegans* dauer larva development. *Nature* 365:644–649.
21. Krishna S, Maduzia LL, Padgett RW (1999) Specificity of TGFbeta signaling is conferred by distinct type I receptors and their associated SMAD proteins in *Caenorhabditis elegans*. *Development* 126:251–260.
22. Savage-Dunn C, et al. (2000) SMA-3 smad has specific and critical functions in DBL-1/SMA-6 TGFbeta-related signaling. *Dev Biol* 223:70–76.
23. Zheng Y, Brockie PJ, Mellem JE, Madsen DM, Maricq AV (1999) Neuronal control of locomotion in *C. elegans* is modified by a dominant mutation in the GLR-1 ionotropic glutamate receptor. *Neuron* 24:347–361.
24. Chalfie M, et al. (1985) The neural circuit for touch sensitivity in *Caenorhabditis elegans*. *J Neurosci* 5:956–964.
25. Gray JM, Hill JJ, Bargmann CI (2005) A circuit for navigation in *Caenorhabditis elegans*. *Proc Natl Acad Sci USA* 102:3184–3191.
26. Piggott BJ, Liu J, Feng Z, Wescott SA, Xu XZ (2011) The neural circuits and synaptic mechanisms underlying motor initiation in *C. elegans*. *Cell* 147:922–933.
27. Macosko EZ, et al. (2009) A hub-and-spoke circuit drives pheromone attraction and social behaviour in *C. elegans*. *Nature* 458:1171–1175.
28. Rand JB, Nonet ML (1997) Synaptic transmission. *Wormbook*, 10.1895/wormbook.1.22.1. Available at http://www.wormbook.org.
29. Mallo GV, et al. (2002) Inducible antibacterial defense system in *C. elegans*. *Curr Biol* 12:1209–1214.
30. Yoshida S, Morita K, Mochii M, Ueno N (2001) Hypodermal expression of *Caenorhabditis elegans* TGF-β type I receptor SMA-6 is essential for the growth and maintenance of body length. *Dev Biol* 240:32–45.
31. Brand T, Schneider MD (1995) Inactive type II and type I receptors for TGF β are dominant inhibitors of TGF β-dependent transcription. *J Biol Chem* 270:8274–8284.
32. Cox GN, Carr S, Kramer JM, Hirsh D (1985) Genetic mapping of *Caenorhabditis elegans* collagen genes using DNA polymorphisms as phenotypic markers. *Genetics* 109: 513–528.
33. Wang J, Tokarz R, Savage-Dunn C (2002) The expression of TGFbeta signal transducers in the hypodermis regulates body size in *C. elegans*. *Development* 129:4989–4998.
34. Nakai J, Ohkura M, Imoto K (2001) A high signal-to-noise Ca(2+) probe composed of a single green fluorescent protein. *Nat Biotechnol* 19:137–141.
35. Ben Arous J, Tanizawa Y, Rabinowitch I, Chatenay D, Schafer WR (2010) Automated imaging of neuronal activity in freely behaving *Caenorhabditis elegans*. *J Neurosci Methods* 187:229–234.
36. Chronis N, Zimmer M, Bargmann CI (2007) Microfluidics for in vivo imaging of neuronal and behavioral activity in *Caenorhabditis elegans*. *Nat Methods* 4:727–731.
37. Ch'ng Q, Sieburth D, Kaplan JM (2008) Profiling synaptic proteins identifies regulators of insulin secretion and lifespan. *PLoS Genet* 4:e1000283.
38. Wang X, et al. (2008) The *C. elegans* L1CAM homologue LAD-2 functions as a coreceptor in MAB-20/Sema2 mediated axon guidance. *J Cell Biol* 180:233–246.
39. Tian C, et al. (2010) The RGM protein DRAG-1 positively regulates a BMP-like signaling pathway in *Caenorhabditis elegans*. *Development* 137:2375–2384.
40. Kunkel MT, Johnstone DB, Thomas JH, Salkoff L (2000) Mutants of a temperature-sensitive two-P domain potassium channel. *J Neurosci* 20:7517–7524.
41. Egan MF, et al. (2003) The BDNF val66met polymorphism affects activity-dependent secretion of BDNF and human memory and hippocampal function. *Cell* 112:257–269.
42. Kang H, Schuman EM (1995) Long-lasting neurotrophin-induced enhancement of synaptic transmission in the adult hippocampus. *Science* 267:1658–1662.
43. Morielli AD, et al. (1986) Cholinergic suppression: A postsynaptic mechanism of long-term associative learning. *Proc Natl Acad Sci USA* 83:4556–4560.
44. Ludwig M, Leng G (2006) Dendritic peptide release and peptide-dependent behaviours. *Nat Rev Neurosci* 7:126–136.